Macromolecules

Article

pubs.acs.org/Macromolecules

Dynamics of DNA Knots during Chain Relaxation

Alexander R. Klotz, Vivek Narsimhan, Beatrice W. Soh, and Patrick S. Doyle*

Department of Chemical Engineering, Massachusetts Institute of Technology, 77 Massachusetts Ave., Cambridge, Massachusetts 02142, United States

Supporting Information

ABSTRACT: We perform single-molecule experiments and simulations to study the swelling of complex knots in linearly extended DNA molecules. We induce self-entanglement of DNA molecules in a microfluidic T-junction using an electrohydrodynamic instability and then stretch the molecules using divergent electric fields. After the chain is fully extended, the knot appears as a region of excess fluorescent brightness, and we shut off the field and observe the knot swelling over time. We find (1) the knot topologies created by the instability are more complex than what is expected from equilibrium simulations of knot formation, (2) the knot swells at a time scale comparable to the end-to-end relaxation of the chain, which indicates that the swelling is dictated by the chain's global dynamics, and (3) knots are long-lived when the DNA is in the coiled state. These findings demonstrate the rich physics involved in the relaxation of knotted polymers which has not been examined heretofore.

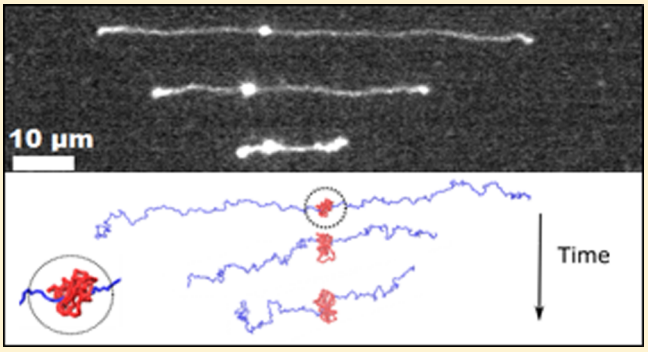

INTRODUCTION

In the past few decades, DNA molecules have been investigated as a model system to study polymer physics at the single-chain level. Their utility as a model polymer arises from their compatibility with fluorescence microscopy, their mesoscopic length scales and time scales, and the monodispersity found in viral genomes. DNA has become the canonical semiflexible polymer to study the polymer physics of stretched chains,[1] the competing roles of self-exclusion and bending rigidity in confinement,[2] and the time scales associated with polymer relaxation.[3−5] Much of the information learned from single-molecule biophysics has been incorporated into emerging genomics technologies such as nanochannel mapping[6] and nanopore sequencing.[7] Typical experiments involve simple topologies such as linear and occasionally circular chains,[8] but in recent years there has been interest in more topologically complex structures such as supercoils,[9] branched chains,[10] and knots.[11]

Knots are inevitable in long polymers; asymptotically long self-avoiding polymers are virtually guaranteed to be knotted.[12] In biological systems, proteins such as topoisomerases prevent DNA from becoming too knotted by selectively crossing the strands.[13] Viruses, which lack these proteins, are known to eject knotted DNA.[14] In nanofluidic genomic applications, knots may be either beneficial or a detriment. Knots have recently been considered as a braking mechanism for nanopore sequencing, which faces a challenge in controlling the speed of the translocating DNA.[15] Computational analyses[16] have shown that certain topologies can slow or jam the translocation of a molecule in a systematic way, which may be useful in developing protocols for genomic analysis using nanopores. In nanochannel genomic mapping, the presence of unwanted knots may skew the apparent distance between fluorescent markers, leading to erroneous results.[6] In this situation, it is desirable to develop a protocol to remove unwanted knots from DNA or prevent their formation.

From a polymer physics standpoint, knots provide a minimal system with which to study chain entanglement, which strongly affects the dynamic,[17] thermal,[18] and mechanical[19] properties of bulk polymer systems. The equilibrium behavior of polymer knots has been the subject of debate, with some authors[20,21] arguing that a relaxed knot will reach a metastable size and tightness, while others[22] have argued against the existence of metastable knots. To understand the dynamics of knotted polymers and the lifetime of their entanglements, we wish to quantify the dynamic time scales associated with single knots in polymer chains.

The relaxation of a stretched, knotted chain has not been studied in detail. When a knotted polyelectrolyte is stretched, the overall chain entropy is reduced, the charged backbone is brought closer to itself, and the knotted core may be bent at length scales shorter than the chain's persistence length. When the tension is released, the chain entropy increases, a portion of the charged backbone repels itself, and the bent molecule unbends, all of which serve to loosen the knot, although this process may be slowed by intramolecular friction inside the knot.[23] As seen previously,[11] knots swell upon relaxation, and in

Received: February 8, 2017
Revised: April 26, 2017
Published: May 8, 2017

DOI: 10.1021/acs.macromol.7b00287
Macromolecules 2017, 50, 4074−4082

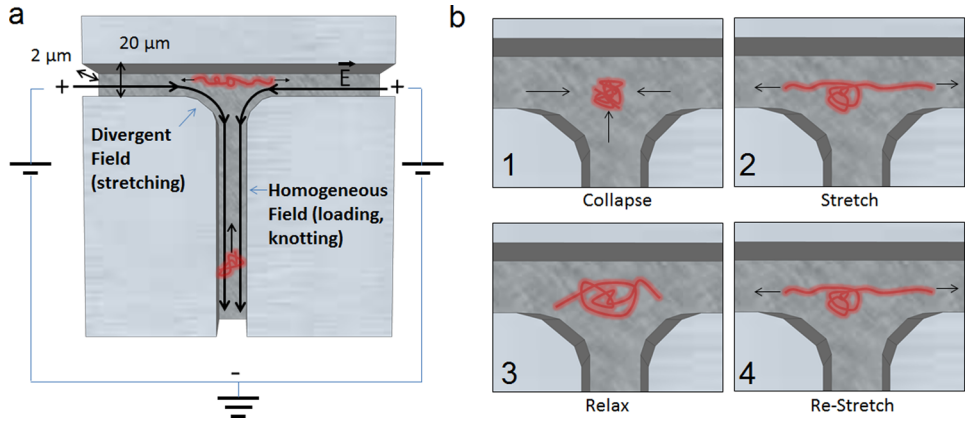

Figure 1. Schematic of the experimental device and protocol. (a) A PDMS microfluidic device with a T-junction contains a divergent electric field that stretches DNA about the device center. (b) DNA molecules are self-entangled using electrohydrodynamic collapse, then stretched, allowed to relax, and restretched repeatedly.

this work we investigate the time scale of this relaxation process.

EXPERIMENTS

Experiments take place in a PDMS microfluidic device with a T-junction geometry with a height of 2 μm and arms of width 20 μm meeting hyperbolically (Figure 1). The device is soaked in 0.5X TBE buffer prior to experiments to prevent permeation driven flow[24] and is laminated onto a glass coverslip. Reservoir holes are punched in the chip to access the microchannel. The device sits atop a 63× oil immersion objective lens on a Zeiss Axiovert inverted microscope, and images are recorded with a Hamamatsu EB-CCD camera, controlled using Micro-Manager.[25] We use T4 GT7 DNA (165.6 kbp), also known in the literature simply as T4, stained with YOYO-1 fluorescent dye at a 4:1 base pair per dye ratio (illuminated with a filtered LED), loaded in a 0.5X TBE buffer with 4% β-mercapotoethanol and 0.1% 10K PVP (polyvinylpyrrolidone). Additionally, we create larger molecules through ligation of λ-DNA by heating a solution of DNA in the presence of the T4 DNA ligase enzyme.

Voltage terminals connected to the reservoirs of the device give rise to an electric field that diverges at the center of the channel, creating a planar extensional field experienced by the charged molecules.[11,26] Molecules can be trapped at the stagnation point and stretched. Two dc voltage supplies are used to create the divergent field, one of which is left at a constant voltage (approximately 30 V) to set the magnitude of the extensional field. The other is set to a similar voltage to create a symmetric field about the midpoint of the T-junction and is toggled manually with shifts on the order of 1 V to balance the field such that the molecule is trapped at the unstable stagnation point. To induce entanglements in the molecule, we exploit an electrohydrodynamic instability investigated previously[27,28] to collapse the molecules into tight globules. It was shown[11] that these tight globules are self-entangled and can trap knots in the interior of the molecule when stretched under an elongational field. In a stretched molecule, a knot appears as a bright region of excess fluorescence because the knotted core contains a greater spatial density of intercalating dye molecules.

When the voltage from both supplies is deactivated, the molecule retracts from a stretched to a coiled state as the overall end-to-end vector decreases in magnitude. During this process, the intensity peak around the knot grows in intensity (Figure 2) until the chain ends overlap with the knot and become indistinguishable from it. A typical experimental assay involves stretching a collapsed self-entangled molecule at the stagnation point, deactivating the voltage, and allowing the molecule to relax back to its coiled state. The field is then reactivated, stretching the molecule back to its extended conformation. The stretch−relax process is repeated until the allotted recording time ends, until photofragmentation destroys the molecule, or until the molecule moves sufficiently far from the stagnation point

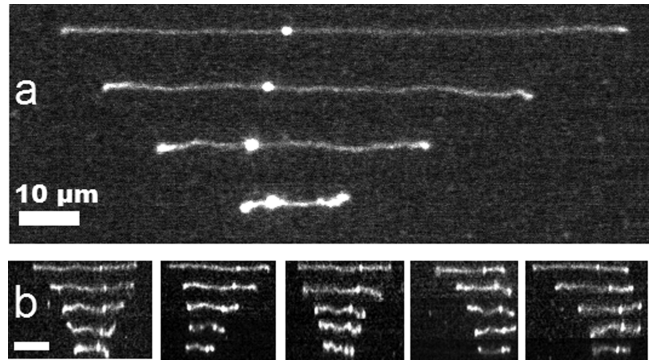

Figure 2. (a) Time series of a large knotted λ-concatemer molecule relaxing. The knot increases in brightness as the end-to-end distance decreases. (b) Five subsequent relaxations of the same T4 molecule, each shown at five time points at 0.6 s intervals from 0 to 2.4 s.

that control is lost. The transient electrohydrodynamic collapse process leads to a stochastic sampling of knots, in that it is unlikely for the same topology to be produced repeatedly. Therefore, stretching multiple molecules gives a sampling of the knots that are produced during the collapse process.

ANALYSIS

All images are processed using home-built MATLAB scripts. In this analysis, we project each image of DNA onto a one-dimensional intensity profile along the chain's backbone and track these intensity profiles over time as a kymograph (Figure 3). An error-function fitting algorithm is adapted from prior DNA studies[29] to identify the ends and extension of the molecule. The knot is identifiable as a bright trajectory on a space-time kymograph and can be located algortihmically as the brighest pixel in the interior of the molecule (Figure 3). The time evolution of the intensity profiles is used to analyze the properties of the knots.

Figure 4a shows the intensity profile along a stretched molecule with two knots of very different excess intensities. We surmise that the brighter knot is significantly more complex topologically. However, it is not apparent that the brighter knot subtends a larger region of the image as both remain unresolved. Indeed, a Gaussian fit to each intensity peak reveals that they have essentially the same full width at half-maximum (fwhm): 1.3 ± 0.1 and 1.5 ± 0.2 μm for the large and small knots, respectively. This is consistent with an experiment

DOI: 10.1021/acs.macromol.7b00287
Macromolecules 2017, 50, 4074−4082

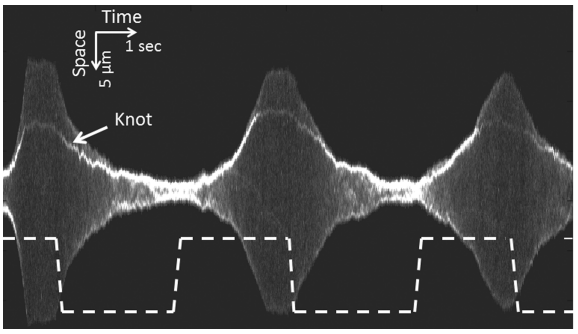

Figure 3. Kymograph of a knotted molecule during the stretch−relax process, oriented about the geometric center of the molecule. As a voltage is applied to the circuit, the molecule stretches, trapping the knot in its interior. As the voltage is deactivated, the molecule relaxes into a coil but the knot remains upon restretching.

from Bao et al.,[30,31] who found that a 17-crossing torus knot could be tightened to a point-like spot. Figures 4b,c show the intensity profile of a single molecule relaxing over time. The apex of the amplitude grows as the knot swells. However, if the peaks are superimposed by normalizing to the apex, again it is seen that they are all of essentially the same width. Because the apparent width of the knot peak is insensitive to both complexity and local tension, it is not an ideal measurable quantity to track the time-evolution behavior of the knot.

While it is difficult to extract information from the apparent width of the knot peak, the amplitude of the peak and its integrated intensity contain a wealth of information about the knot's dynamics. In Figure 4a, for example, we can see that the larger knot has a fluorescent amplitude roughly 6 times greater than that of the small knot. In Figure 4b, the intensity of the peak is seen growing 3-fold as the knot swells. To track the intensity of the knot over time, we define a quantity termed the knot fraction (KF), which is the integrated intensity of the knotted region (i.e., the brightest pixel of the knot plus 3 pixels on each side) divided by the total integrated intensity of the molecule.

$$\mathrm{KF} = \frac{I_{\mathrm{knot}}}{I_{\mathrm{molecule}}} \tag{1}$$

The 7-pixel band defined here is consistent with the width of the knot determined by Gaussian fits using full width at half-maximum. As the molecule relaxes, the arms retract toward the knotted core, and it eventually becomes impossible to distinguish the arms from the knot, at which point our analysis ends. We emphasize that the knot fraction as defined here is not necessarily meant to capture the entirety of the knot's fluorescent intensity, but rather be used as a parameter capable of tracking trends in the contour stored in the knot. The sensitivity of the metric to the size of the window is discussed in the Supporting Information (see Figure S1).

RESULTS

Statics. Before examining the relaxation process of stretched knots, we consider the static properties of knots in our experimental system. The sizes of DNA knots previously measured in the literature are summarized in Table 1. We

Table 1. Estimates of DNA Knot Contour Lengths from the Literature

reference	formation method	knot contour length (nm)
Bao[30]	optical tweezers	200−500
Plesa[34]	equilibrium	<300
Metzler[35]	nanochannel compaction	1800
Reifenberger[6]	nanochannel insertion	1500
Renner[11]	electrohydrodynamic collapse	1000−3000

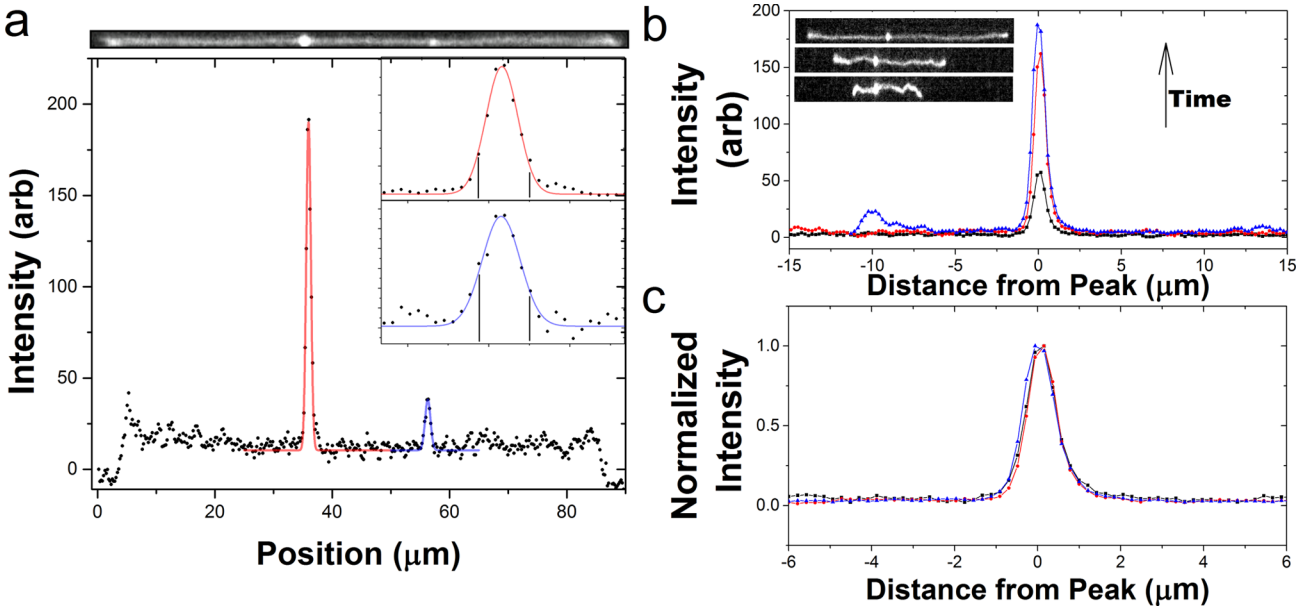

Figure 4. (a) Fluorescence micrograph and intensity profile of a molecule with two knots of different size. While the integrated intensity in the large knot is 6 times greater, the apparent widths of the knots are comparable. Gaussian fits to the knot intensity peaks (red, blue) yield similar full widths at half-maximum (1.3 ± 0.1 μm for the large knot and 1.5 ± 0.2 μm for the small knot). The vertical lines in the insets show the 7-pixel window used to track the integrated knot intensity. (b, c) One knot in a relaxing molecule at three time points. The knot grows in intensity, but the width of the peak remains unchanged.

DOI: 10.1021/acs.macromol.7b00287
Macromolecules 2017, 50, 4074−4082

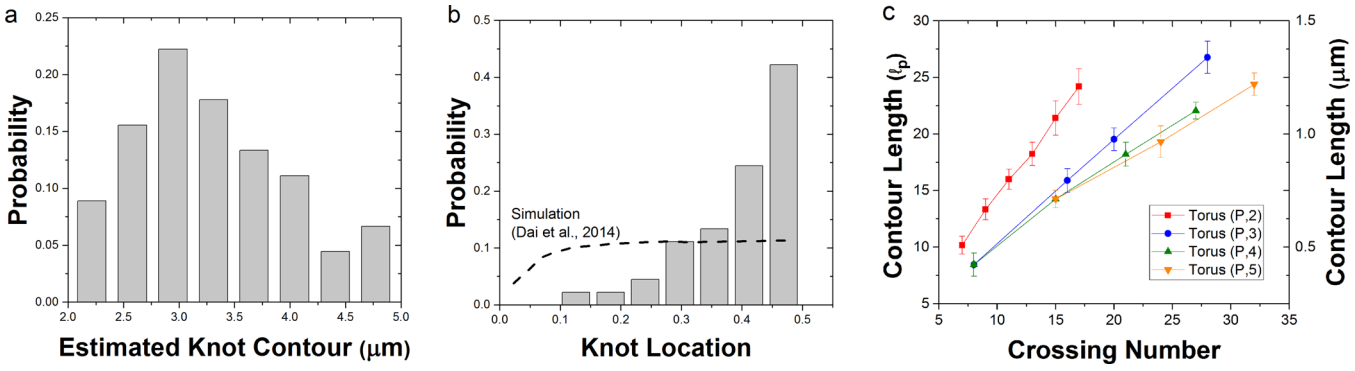

Figure 5. (a) Histogram of estimated knot contour lengths from an ensemble of 45 T4 molecules stretched at steady-state at Wi = 2.9 (one measurement per molecule). The estimated contours are much greater than those of the simple knots seen by Bao et al.,[30] and the skew of the distribution deviates from equilibrium simulations of knot formation.[32] (b) Histogram of the location of knots along molecule, imposing 2-fold symmetry. They are more likely to found near the middle, but it is unknown if this observation is due to the formation or the initial stretching of the knots. The dashed line shows the prediction of an equilibrium simulation from our group.[21] (c) Brownian dynamics simulations of knot sizes for various torus topologies at tension f = 0.82 pN typically experienced at the center of DNA in experiments (i.e., Wi = 2.9 in planar extensional field). The sizes are in units of persistence lengths of dsDNA (l_p = 50 nm), and the error bars are standard deviations. More details of the simulations are in the Supporting Information.

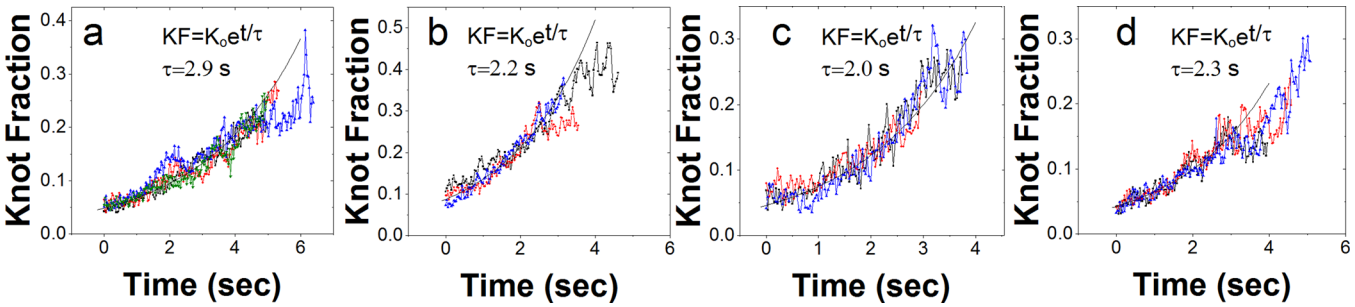

Figure 6. Knot growth trajectories of four molecules each making at least three relaxations. Exponential fits are shown, fit to the 65 time points between 0.5 and 2.5 s. Part a shows four relaxations, and parts b–d show three.

examine the steady-state ensemble of 45 molecules stretched in an elongational field at Weissenberg number Wi = 2.9, where $Wi = \dot{\epsilon}\lambda$ is the product of the extension rate $\dot{\epsilon}$ and the longest stress relaxation time λ of the molecule. Figure 5a shows a histogram of the contour inside the knot, which we measure as the product of the knot fraction with the total chain length (L), taken to be 75 μm for maximally stained T4.[11] The knot contour distribution has a peak at 3 μm, which is comparable to the difference in the end-to-end extension between knotted and unknotted molecules created by our electrohydrodynamic instability.[11] These measured contour lengths are significantly greater than those measured in 3–7 crossing knots created by optical tweezers (Table 1).[30] Furthermore, the distribution of knot sizes is different than equilibrium simulations of knotted polymers,[32] which state that 3-crossing trefoil knots are overwhelmingly common in T4 DNA. These results suggest that the knots created in our experimental setup are much more complex than those created from equilibrium processes, and we hypothesize that the same is true for knots produced by nanochannel insertion by Bionano Genomics.[6] We performed Brownian dynamics simulations (Figure 5c) to determine the knot size of various topologies under tensions that are comparable to the tensions found at the center of DNA in our experiments. We see that for knots to contain over 1 μm of contour in our experimental conditions, torus knots must contain dozens of crossings, and there are many possible topologies for a given size of knot. We note that comparably complex topologies have been observed in simulations of strongly collapsed polymers in poor solvent,[33] which is not the same as our electrohydrodynamic collapse but exhibits similarities in terms of overall polymer conformation. Lastly, in Figure 5b we plot the distribution of knots along the chain contour, showing that they are most likely found near the center of the molecule but rarely near the end. While theoretical analysis shows[21] a small bias toward centrally located knots, the observed central tendency is much greater in our experiments. We cannot ascertain whether this observation is due to the knot formation mechanism, the initial stretching process, or the tendency of knots near the end to untie themselves before visualization.

Relaxation Dynamics. An example of the knot fraction measured during swelling is seen in Figure 6, which shows knot growth trajectories on four different molecules making at least three relaxations. For each molecule, the knot growth appears similar between different relaxations, which indicates that the measurements are repeatable. To measure the characteristic time scale of knot growth, we perform an exponential fit to the 65 time points between 0.5 and 2.5 s in the knot growth trajectory, chosen to avoid the initial perturbation of deactivating the electric field as well as the late-time behavior when the molecule ceases to be effectively straight or the ends of the chain overlap the knot.

Figure 7 shows the relationship between the measured knot growth time scale and the apparent size of the knots for an ensemble of T4 molecules measured at a common extension. The mean knot time scale was found to be 2.7 ± 0.1 s. The

DOI: 10.1021/acs.macromol.7b00287
Macromolecules 2017, 50, 4074–4082

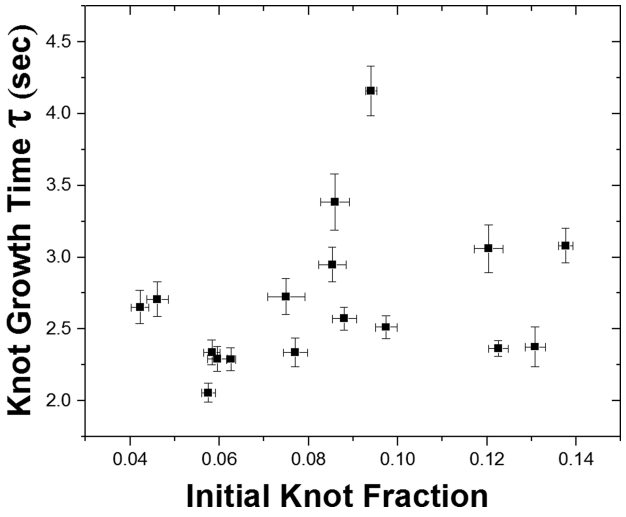

Figure 7. Scatter plot of the characteristic knot growth time scale of 17 molecules and the estimated size of their knots at a common extension of 45%. Error bars represent the standard error as measured over multiple relaxation events, at least three per molecule.

variation in the time scales across the ensemble is around 50%, while the variation in the size of the knot is around 300%. There is no apparent correlation between the size of a knot and its growth time scale. To the extent that a positive correlation does exist (implying larger knots relax more slowly), it is not statistically significant with a *p*-value of 0.27 based on Pearson's coefficient, and 0.22 if the strongest outlier is omitted. Indeed, the data suggest that the time scale of the knot is insensitive to its topological complexity.

The sensitivity of knot growth dynamics to the topological complexity can be further probed by examining the relaxation behavior of molecules with two knots of differing complexity. Such a system is beneficial because the underlying relaxation dynamics of the chain drives the swelling of both knots simultaneously. An example is seen in Figure 8, showing that two knots of differing brightness relax similarly, with a ratio between the two intensities that does not change significantly over time.

If the knot growth time scale is insensitive to topology, then what determines the time scale? Inspired by the fact that the measured time scale is comparable to the characteristic end-to-end relaxation time of T4 DNA molecules,[3] we posit that the knot growth time scale is governed by the same physics as the end-to-end retraction time scale, implying that the contour in the knot increases at the same time scale as the extended arms decrease in length. To establish equivalency between these two time scales, we define a dimensionless parameter termed the knot product, which is the fraction of total fluorescent intensity within the knot multiplied by the fractional extension of the molecule, defined below and described schematically in Figure 9a:

$$P(t) \equiv \frac{I_{\mathrm{knot}}(t)}{I_{\mathrm{tot}}}\frac{L_{\mathrm{ee}}(t)}{L_{\mathrm{c}}} \approx \frac{L_{\mathrm{knot}}(t)L_{\mathrm{ee}}(t)}{{L_{\mathrm{c}}}^2} \qquad (2)$$

where L_c is the total contour length of the molecule, L_{ee} is the end-to-end extension of the molecule, and L_{knot} is the contour length within the knot (to which I_{knot} is assumed to be proportional). This parameter is sensitive to differences between the overall relaxation behavior of the molecule and the swelling of the knot. An example is shown in Figure 9b,

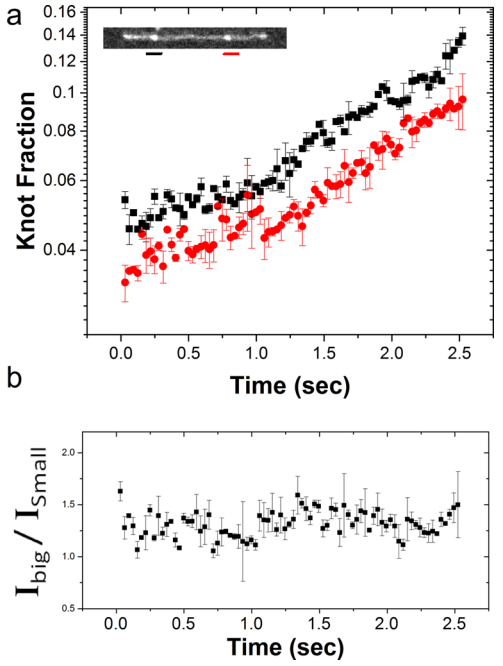

Figure 8. (a) Knot fractions (KF) of two knots on the same molecule as the molecule relaxes. (b) The ratio between the two intensities, which is roughly constant over time. Error bars represent the uncertainty as measured over two relaxation events.

showing the relative extension, knot fraction, and their product as a function of time. The upward growth of the knot and downward shrinking of the extension appear to have the same exponential slope, and their product, though subject to fluctuations, is unchanging over time. Figure 9c shows the time evolution of this product for a single relaxation, several relaxations averaged over a single molecule, and several relaxations averaged over an ensemble of molecules. While perhaps trends can be seen in the smoother curves, the product is essentially constant over time with variation below 20%. The flatness of these curves at the relaxation, molecule, and ensemble level suggest that overall there are no significant differences in the time scales of knot growth and knot relaxation.

Our position can be further verified by examining the relaxation of knots in molecules longer than T4 DNA (Figure 10). If our hypothesis is correct, there would be a correspondence between the end-to-end relaxation time and the knot growth time for molecules of any length. This would also refute the unlikely case that the characteristic growth time of all knots is uniform and happens to be similar to the end-to-end relaxation time of T4 DNA. To this end, we perform an experiment using concatemers of λ DNA, which have a size distribution over a wide range and can be significantly larger than T4 DNA. While the individual size of a molecule is not known precisely (nor is the Weissenberg number it is experiencing), the correspondence between the two time scales can be examined. It is found that even for larger molecules, the end-to-end relaxation time as measured by an exponential fit is comparable to the growth time of the knot, although the latter is a significantly noisier measurement. We also attempt to examine smaller chains by examining T4 molecules that have undergone photofragmentation. Overall, this data lends further credence to the fact that the two time scales are dominated by the same underlying physics.

DOI: 10.1021/acs.macromol.7b00287
Macromolecules 2017, 50, 4074−4082

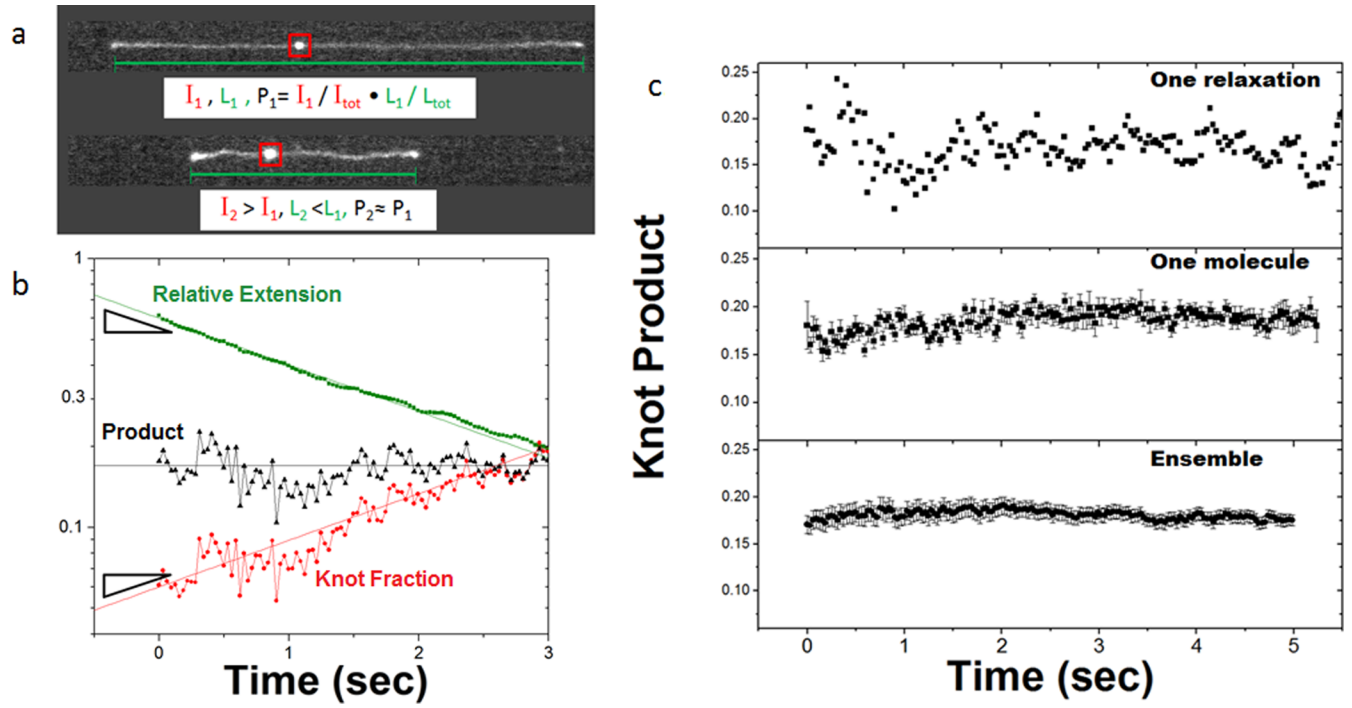

Figure 9. (a) The knot product is defined as the relative extension of the molecule multiplied by the fraction of intensity within the knot. This diagram explains its measurement at two time points. (b) Relative extension, knot fraction, and knot product over time for a single relaxation. The magnitude of the slopes of the exponentially growing fit to the knot fraction and exponentially decaying fit to the extension are the same. (c) Knot product over time for a single relaxation, for 13 relaxations in a single molecule, and an ensemble of 17 multiply relaxing T4 molecules. The product does not evolve significantly over time. Error bars represent the standard error as measured over multiple relaxations (b) and multiple molecules (c).

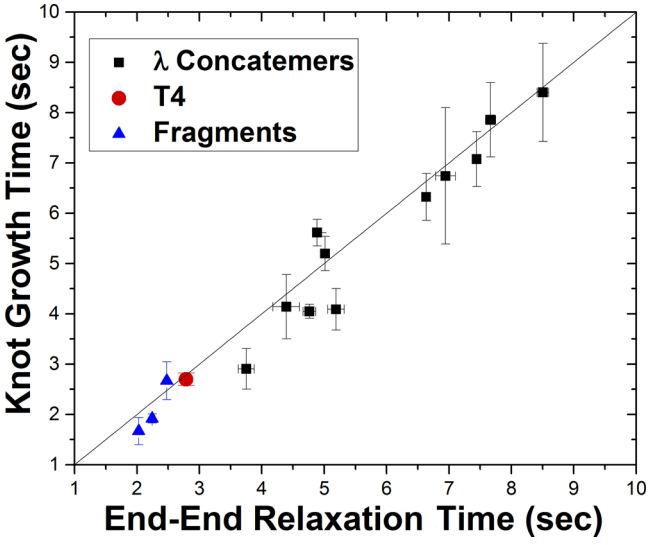

Figure 10. Scatter plot of the characteristic knot time scale and the end-to-end relaxation time for molecules of varying size, ranging from fragmented sub-T4 molecules to an ensemble of 17 T4 molecules to much larger concatemers of λ DNA. The line represents equality between the two time scales, and the measurements are distributed about it. Error bars represent standard confidence intervals of exponential fits to single relaxations.

SIMULATIONS

We perform Brownian dynamics (BD) simulations to further explore two major findings from our experiments: that the knot growth time scale is related to the global relaxation time scale of the chain and that the knot growth process is insensitive to topology. A schematic of our simulation is shown in Figure 11a.

We represent our polymer as a flexible chain of connected beads of size b with a drag coefficient of ζ on each bead. We tie a knot into the center of the chain, apply a tension f at both ends, and wait until the knot has equilibrated. We then turn off the force and track the knot size as a function of time as it swells. By varying the chain length and the knot topology, we can explore explore how these factors affect the swelling behavior of the knot. Results from our simulations are shown below. Further details of the simulation protocol are discussed in the Supporting Information (see Figure S4).

Figure 11a shows the swelling of a trefoil (3_1) knot as a function of time for different chain lengths (N = 400−700 beads). We see that the knot swells more slowly when the chain is longer. However, if we normalize time by the relaxation time λ of the chain, the swelling profiles collapse onto each other (Figure 11b). Here, we define the relaxation time λ from the long-time, exponential decay of the mean-squared end-to-end distance of the stretched, unknotted polymer chain: $\langle L_{ee}(t)^2 \rangle \sim \exp(-t/\lambda)$. We note that a similar collapse occurs for other knot topologies such as the 10-crossing knot (10_1) (Figure 11b). These results suggest that the knot swelling is slaved to the global relaxation of the chain rather than local dynamics within the knotted core. These observations are also consistent with the experimental findings that the knot swelling time is commensurate to the end-to-end relaxation time, which is 2λ as defined here.

In Figure 11c, we determine how the knot swelling time scale varies with chain topology for a wide variety of knot types. We calculate the knot swelling time scale as follows. When a knot swells from an initially extended chain, our experiments suggest that the knot size $S(t)$ increases with time as

$$S(t) = S(0) \exp\{\alpha(t/\lambda)\} \quad (3)$$

DOI: 10.1021/acs.macromol.7b00287
Macromolecules 2017, 50, 4074−4082

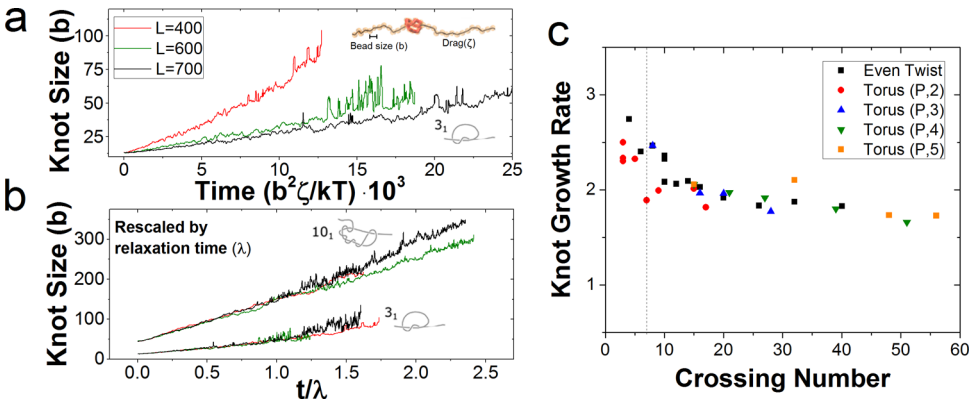

Figure 11. Brownian dynamics simulations of a knot swelling on an extended chain. We represent a polymer as a flexible chain of touching beads of size b with drag coefficient ζ. (a) Knot swelling as a function of time for a 3_1 knot with different chain lengths. Curves are averages over 20 runs, and the initial tension is $f = 5kT/b$. (b) Knot growth data rescaled by the chain relaxation time λ of the unknotted chain. Trajectories are shown for the 3_1 and 10_1 knots. (c) Normalized knot swelling time scale α as defined by eq 3 for various knot topologies defined in the Supporting Information. Results are averages over 10−20 runs with initial tension $f = 5kT/b$. For torus $(p, 2)$ knots and even twist (n) knots with 10 or fewer crossings, we simulated $N = 400$ bead chains. For the remaining topologies, we simulated $N = 600$ bead chains. We also include results for $N = 400$, 600, and 700 bead chains for the 3_1 and 10_1 topologies. The dashed vertical line shows the typical range of knot topologies considered in the literature.[20]

where λ is the chain relaxation time and α is the normalized knot swelling rate. We calculate α in our simulations as the slope of $S(t/\lambda)/S(0)$ at normalized time $t/\lambda = 0$ and plot the results for different knot topology families in Figure 11c. We observe that the normalized swelling rate decreases with increasing knot complexity but falls very slowly beyond 10 crossings. This result suggests that as the knot becomes very complex, the swelling behavior becomes insensitive to topology, which provides an explanation as to why we observe similar knot swelling profiles in experiments even though we stochastically sample different knot types. Many quantitative differences between experiments and simulations can be attributed to the fact that the simulations are not parametrized to DNA and do not take hydrodynamic interactions into account in the knotted core, which would certainly play a role in modifying knot swelling. The fact we are able to capture the major trends found in experiments via a minimalistic, general polymer model indicates that the knot dynamics we observe is likely to be found during the relaxation of all stretched polymer chains.

DISCUSSION

In studying the relaxation of a stretched, knotted chain, we have concluded that knots swell at a time scale that is dominated by the global relaxation dynamics of the chain, and these dynamics are insensitive to the topology of the knot (at least for sufficiently complex topologies). While some aspects of knot dynamics have been examined computationally, prior to this work there have not been detailed simulations on the knot relaxation process. The closest extant study is that of Zheng and Vologodskii,[22] who simulated the relaxation of a stretched 7-crossing knot. In agreement with our results, they found that the growth rate of the knot depends on the overall length of the chain, but expansion of other topologies was not probed. Another study was that of Lai et al.,[36] who introduced a "cut" into an *untensed* circular knotted chain and examined the relaxation of the radius of gyration toward the unknotted equilibrium value. They found that the knot relaxation time increases with complexity (as characterized by the rope length) and is further characterized by the parity of the crossing number and grouped into classes based on the topological subtype.

Our simulations support the claims that the knot growth time scale is dictated by global dynamics and is insensitive to topology. The former is evidenced by the fact the rescaling by the global relaxation time causes different species of chain with the same knot to have the same knot growth dynamics (Figure 11b). The latter is evidenced by the fact that the characteristic knot growth rates plateau as the knots become sufficiently complex (Figure 11c), beyond ten crossings. Earlier studies[30,36] had only probed simpler knots, where topology dependence is stronger.

While differences remain between the experiments and the simulations (which were not parametrized to encapsulate exactly the properties of DNA), they support our conclusions that the knot swelling time scale is determined by global dynamics and is insensitive to topology. We note that other dynamical processes such as diffusion[30] have stronger topological dependence, due to the self-reptation through the knot core that is required. If knot swelling does indeed depend on knot type, this dependence is likely manifested at time scales shorter than those we are able to probe or becomes relevant at tensions greater than those experienced by the molecules in our experiments. We also expect that for short chains the correspondence between the two time scales breaks down. Our experiments examine the swelling dynamics on a *stretched* chain. It is an open question whether the time scale of knot fluctuations in a coiled chain (for example, the process studied by Orlandini et al.[37]) depends on knot complexity.

Our experimental results indicate that we are sampling very large knots, in the regime found in our simulations where knot dynamics are insensitive to topology. This is consistent with our analysis of steady-state knot sizes (Figure 5a), which reveals a distribution of knots that has a peak in the middle range of observed sizes, rather than the smallest knots. Indeed, the knot contour lengths ascertained by analyzing the intensity, as well as a similar measurement of the difference in extension between knotted and unknotted molecules, suggest that the typical knot contains over 2 μm of contour, which is significantly greater than the typical contour stored in simple knots (three through seven crossings). Measurements of DNA knot size in the

DOI: 10.1021/acs.macromol.7b00287
Macromolecules 2017, 50, 4074−4082

literature (Table 1) suggest that knots formed through nonequilibrium methods bear significantly more contour than the simplest knots. To estimate the topological complexity of our observed knots, we performed simulations of complex knots at steady-state tension in chains that were parametrized to have DNA's properties (Figure 5c). It was found that even knots with over 30 crossings are expected to contain less than 2 μm of contour, suggesting that our knots have crossing numbers in the dozens. Since equilibrium simulations[32] predict that trefoil knots are by far the most likely to occur, this result strongly suggests that nonequilibrium compaction greatly enhances the complexity of knots. While no simulation of such dynamic knot formation currently exists, we draw analogy to the analysis of Mansfield,[33] who found that in the case of a strongly self-attracting polymer 60% of detected knots at equilibrium had more than 10 crossings. As of now, we posit that knots form from electrohydrodynamic collapse when dense aggregates of contour are penetrated by the ends of the chain. This is supported by observations of the instability of pre-extended molecules, which causes only the chain ends to collapse into tight globules, which can be stretched to reveal a knot close to each end of the molecule. Further investigation into nonequilibrium knot formation processes would be helpful in understanding how these very complex knots are formed.

While it is not the primary focus of this work, our experiments may have implications for the metastable knot controversy:[20,22] in a sense, our experiments would be impossible without long-lived knots. When our molecules relax to the coiled state, the knots remain present upon restretching, implying at the very least that the knot did not swell to the point of untying itself. In experiments, the molecules typically only diffuse in the coiled state for a few seconds before we restretch them. To test the limits of knot persistence, a knotted molecule was allowed to diffuse freely in its coiled state for 2 min (~100 chain relaxation times), and the knot remained in the interior of the molecule (see Figure S3). Although preliminary, this observation is suggestive of the existence of metastable knots or very slow unknotting kinetics, and future work will examine the behavior of knot persistence and untying using the knot-stretch−coil-stretch assay.

There are other polymer aggregation phenomena besides knots that would give the appearance of bright peaks along the chain, but we do not suspect that knot mimicry is an issue. If the excess brightness is caused by proteins that were not sufficiently removed from the DNA during its purification, we would see peaks without applying the collapsing field. If the peaks were caused by regions of tight folds caused by latent self-attraction from the collapse process, we would expect that if they were sufficiently stretched to the point of being invisible, they would not re-form when the tension is released, and we would expect these to spontaneously decrease in brightness. Knots can vanish below the noise floor if enough tension is applied, but they re-emerge in the same location when the tension is released. Supercoils that are kinetically constrained from unraveling, or simple knots containing supercoils, would give the appearance of bright peaks, but again we would expect these to dissipate over time, especially if single-strand nicks were induced by the excitation light. One possibility is that the knots are pseudoknots formed by entangled hernia loops, similar to what was observed in stretched circular DNA,[38] but it was shown that such pseudoknots could be tightened out of existence at Wi = 1.9, whereas our knots survive under Wi = 5. Additionally, we have observed our suspected knots reach the end of the chain and untie themselves. Additional consideration of whether knots are indeed forming can be found in our previous discussions on the topic.[11,27]

CONCLUSION

We have made quantitative measurements of the swelling process of complex knots in initially stretched DNA molecules. Our results reveal that for the large knots that we sample the knots grow at a rate dictated by the global relaxation process of the molecule without significant dependence on the complexity of the knot. These findings are supported by Brownian dynamics simulations of the knot relaxation process. Lastly, we find that these large knots are long-lived when DNA is in the coiled state. We hope that this paper drives interest into the mathematical and physical understanding of knots that are significantly more complex than the simplest species that are usually studied.

ASSOCIATED CONTENT

Supporting Information

The Supporting Information is available free of charge on the ACS Publications website at DOI: 10.1021/acs.macromol.7b00287.

Additional details regarding the experimental analysis, the lifetime of knots, and simulation algorithms (PDF)

AUTHOR INFORMATION

Corresponding Author

*E-mail: pdoyle@mit.edu (P.S.D.).

ORCID

Alexander R. Klotz: 0000-0002-1581-6956

Notes

The authors declare no competing financial interest.

ACKNOWLEDGMENTS

The authors thank Dai Liang for his helpful comments and are especially grateful to C. Benjamin Renner for his advice. This research was supported by the National Research Foundation Singapore through the Singapore MIT Alliance for Research and Technology's research program in BioSystems and Micromechanics and the National Science Foundation (Grant CBET-1602406). A.R.K. is funded by an NSERC Postdoctoral Fellowship.

REFERENCES

(1) Marko, J. F.; Siggia, E. D. Stretching DNA. *Macromolecules* **1995**, *28*, 8759−8770.

(2) Klotz, A. R.; Duong, L.; Mamaev, M.; de Haan, H. W.; Chen, J. Z.; Reisner, W. W. Measuring the confinement free energy and effective width of single polymer chains via single-molecule tetris. *Macromolecules* **2015**, *48*, 5028−5033.

(3) Balducci, A.; Hsieh, C.-C.; Doyle, P. Relaxation of stretched DNA in slitlike confinement. *Phys. Rev. Lett.* **2007**, *99*, 238102.

(4) Klotz, A. R.; Mamaev, M.; Duong, L.; de Haan, H. W.; Reisner, W. W. Correlated Fluctuations of DNA between Nanofluidic Entropic Traps. *Macromolecules* **2015**, *48*, 4742−4747.

(5) Klotz, A. R.; de Haan, H. W.; Reisner, W. W. Waves of DNA: Propagating excitations in extended nanoconfined polymers. *Phys. Rev. E: Stat. Phys., Plasmas, Fluids, Relat. Interdiscip. Top.* **2016**, *94*, 042603.

(6) Reifenberger, J. G.; Dorfman, K. D.; Cao, H. Topological events in single molecules of E. coli DNA confined in nanochannels. *Analyst* **2015**, *140*, 4887−4894.

DOI: 10.1021/acs.macromol.7b00287
Macromolecules 2017, 50, 4074−4082

(7) Judge, K.; Harris, S. R.; Reuter, S.; Parkhill, J.; Peacock, S. J. Early insights into the potential of the Oxford Nanopore MinION for antimicrobial resistance gene detection, 2015.
(8) Lin, P.-k.; Hsieh, C.-C.; Chen, Y.-L.; Chou, C.-F. Effects of topology and ionic strength on double-stranded DNA confined in nanoslits. *Macromolecules* **2012**, *45*, 2920−2927.
(9) van Loenhout, M. T.; de Grunt, M.; Dekker, C. Dynamics of DNA supercoils. *Science* **2012**, *338*, 94−97.
(10) Mai, D. J.; Marciel, A. B.; Sing, C. E.; Schroeder, C. M. Topology-controlled relaxation dynamics of single branched polymers. *ACS Macro Lett.* **2015**, *4*, 446−452.
(11) Renner, C. B.; Doyle, P. S. Stretching self-entangled DNA molecules in elongational fields. *Soft Matter* **2015**, *11*, 3105−3114.
(12) Sumners, D.; Whittington, S. Knots in self-avoiding walks. *J. Phys. A: Math. Gen.* **1988**, *21*, 1689.
(13) Rybenkov, V. V.; Ullsperger, C.; Vologodskii, A. V.; Cozzarelli, N. R. Simplification of DNA topology below equilibrium values by type II topoisomerases. *Science* **1997**, *277*, 690−693.
(14) Liu, L. F.; Perkocha, L.; Calendar, R.; Wang, J. C. Knotted DNA from bacteriophage capsids. *Proc. Natl. Acad. Sci. U. S. A.* **1981**, *78*, 5498−5502.
(15) Narsimhan, V.; Renner, C. B.; Doyle, P. S. Translocation dynamics of knotted polymers under a constant or periodic external field. *Soft Matter* **2016**, *12*, 5041−5049.
(16) Suma, A.; Rosa, A.; Micheletti, C. Pore Translocation of Knotted Polymer Chains: How Friction Depends on Knot Complexity. *ACS Macro Lett.* **2015**, *4*, 1420−1424.
(17) Likhtman, A. E.; McLeish, T. C. Quantitative theory for linear dynamics of linear entangled polymers. *Macromolecules* **2002**, *35*, 6332−6343.
(18) De Gennes, P. G. Tight knots. *Macromolecules* **1984**, *17*, 703−704.
(19) Saitta, A. M.; Soper, P. D.; Wasserman, E.; Klein, M. L. Influence of a knot on the strength of a polymer strand. *Nature* **1999**, *399*, 46−48.
(20) Grosberg, A. Y.; Rabin, Y. Metastable tight knots in a wormlike polymer. *Phys. Rev. Lett.* **2007**, *99*, 217801.
(21) Dai, L.; Renner, C. B.; Doyle, P. S. Metastable Tight Knots in Semiflexible Chains. *Macromolecules* **2014**, *47*, 6135−6140.
(22) Zheng, X.; Vologodskii, A. Tightness of knots in a polymer chain. *Phys. Rev. E* **2010**, *81*, 041806.
(23) Narsimhan, V.; Renner, C. B.; Doyle, P. S. Jamming of Knots along a Tensioned Chain. *ACS Macro Lett.* **2016**, *5*, 123−127.
(24) Randall, G. C.; Doyle, P. S. Permeation-driven flow in poly (dimethylsiloxane) microfluidic devices. *Proc. Natl. Acad. Sci. U. S. A.* **2005**, *102*, 10813−10818.
(25) Edelstein, A. D.; Tsuchida, M. A.; Amodaj, N.; Pinkard, H.; Vale, R. D.; Stuurman, N. Advanced methods of microscope control using μManager software. *Journal of Biological Methods* **2014**, *1* (2), e11.
(26) Tang, J.; Doyle, P. S. Electrophoretic stretching of DNA molecules using microscale T junctions. *Appl. Phys. Lett.* **2007**, *90*, 224103.
(27) Tang, J.; Du, N.; Doyle, P. S. Compression and self-entanglement of single DNA molecules under uniform electric field. *Proc. Natl. Acad. Sci. U. S. A.* **2011**, *108*, 16153−16158.
(28) Zhou, C.; Reisner, W. W.; Staunton, R. J.; Ashan, A.; Austin, R. H.; Riehn, R. Collapse of DNA in AC electric fields. *Phys. Rev. Lett.* **2011**, *106*, 248103.
(29) Reisner, W.; Morton, K. J.; Riehn, R.; Wang, Y. M.; Yu, Z.; Rosen, M.; Sturm, J. C.; Chou, S. Y.; Frey, E.; Austin, R. H. Statics and dynamics of single DNA molecules confined in nanochannels. *Phys. Rev. Lett.* **2005**, *94*, 196101.
(30) Bao, X. R.; Lee, H. J.; Quake, S. R. Behavior of complex knots in single DNA molecules. *Phys. Rev. Lett.* **2003**, *91*, 265506.
(31) Lee, H. J. Personal communication.
(32) Rieger, F. C.; Virnau, P. A Monte Carlo study of knots in long double-stranded DNA chains. *PLoS Comput. Biol.* **2016**, *12*, e1005029.
(33) Mansfield, M. L. Development of knotting during the collapse transition of polymers. *J. Chem. Phys.* **2007**, *127*, 244902.
(34) Plesa, C.; Verschueren, D.; Pud, S.; van der Torre, J.; Ruitenberg, J. W.; Witteveen, M. J.; Jonsson, M. P.; Grosberg, A. Y.; Rabin, Y.; Dekker, C. Direct observation of DNA knots using a solid-state nanopore. *Nat. Nanotechnol.* **2016**, DOI: 10.1038/nnano.2016.153.
(35) Metzler, R.; Reisner, W.; Riehn, R.; Austin, R.; Tegenfeldt, J.; Sokolov, I. M. Diffusion mechanisms of localised knots along a polymer. *EPL (Europhysics Letters)* **2006**, *76*, 696.
(36) Lai, P.-Y.; Sheng, Y.-J.; Tsao, H.-K. Structure and relaxation dynamics of polymer knots. *Phys. A* **2000**, *281*, 381−392.
(37) Orlandini, E.; Stella, A. L.; Vanderzande, C.; Zonta, F. Slow topological time scale of knotted polymers. *J. Phys. A: Math. Theor.* **2008**, *41*, 122002.
(38) Li, Y.; Hsiao, K.-W.; Brockman, C. A.; Yates, D. Y.; Robertson-Anderson, R. M.; Kornfield, J. A.; San Francisco, M. J.; Schroeder, C. M.; McKenna, G. B. When ends meet: Circular DNA stretches differently in elongational flows. *Macromolecules* **2015**, *48*, 5997−6001.

DOI: 10.1021/acs.macromol.7b00287
Macromolecules 2017, 50, 4074−4082